Front. Environ. Sci. Eng. 2019, 13(4): 59
https://doi.org/10.1007/s11783-019-1143-2

RESEARCH ARTICLE

Ozonation of the 5-fluorouracil anticancer drug and its prodrug capecitabine: Reaction kinetics, oxidation mechanisms, and residual toxicity

Siyu Chen[1], Lee Blaney[1,2], Ping Chen[1], Shanshan Deng[1], Mamatha Hopanna[2], Yixiang Bao[1], Gang Yu (✉)[1]

1 School of Environment, State Key Joint Laboratory of Environmental Simulation and Pollution Control (SKLESPC), Beijing Key Laboratory for Emerging Organic Contaminants Control, Tsinghua University, Beijing 100084, China
2 Department of Chemical, Biochemical, and Environmental Engineering, University of Maryland Baltimore County, Baltimore, MD 21250, USA

HIGHLIGHTS

- Specific second-order rate constants were determined for 5-FU and CAP with ozone.
- Reaction sites were confirmed by kinetics, Fukui analysis, and products.
- The olefin moiety was the main ozone reaction site for 5-FU and CAP.
- Carboxylic acids comprised most of the residual TOC for 5-FU.
- Ozonation removed the toxicity associated with 5-FU and products but not CAP.

ARTICLE INFO

Article history:
Received 3 April 2019
Revised 1 May 2019
Accepted 15 May 2019
Available online 24 June 2019

Keywords:
Ozone
5-fluorouracil
Capecitabine
Hydroxyl radicals
Chemotherapy agents
Toxicity

GRAPHIC ABSTRACT

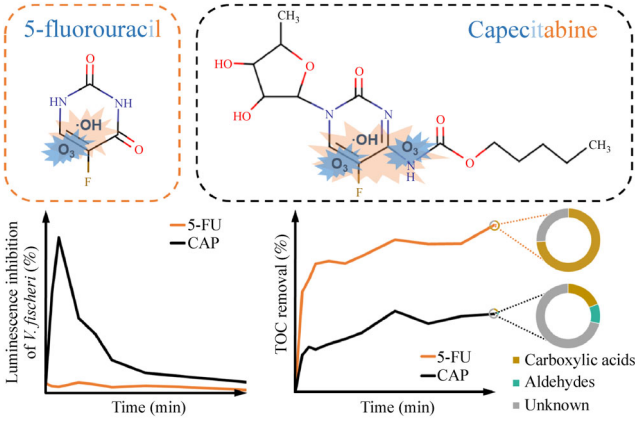

ABSTRACT

Anticancer drugs (ADs) have been detected in the environment and represent a risk to aquatic organisms, necessitating AD removal in drinking water and wastewater treatment. In this study, ozonation of the most commonly used antimetabolite ADs, namely 5-fluorouracil (5-FU) and its prodrug capecitabine (CAP), was investigated to determine reaction kinetics, oxidation mechanisms, and residual toxicity. The specific second-order rate constants between aqueous ozone and 5-FU, 5-FU^-, 5-FU^{2-}, CAP, and CAP^- were determined to be $7.07(\pm0.11)\times10^4$ $M^{-1}\cdot s^{-1}$, $1.36(\pm0.06)\times10^6$ $M^{-1}\cdot s^{-1}$, $2.62(\pm0.17)\times10^7$ $M^{-1}\cdot s^{-1}$, $9.69(\pm0.08)\times10^3$ $M^{-1}\cdot s^{-1}$, and $4.28(\pm0.07)\times10^5$ $M^{-1}\cdot s^{-1}$, respectively; furthermore, the second-order rate constants for $^{\bullet}OH$ reaction with 5-FU and CAP at pH 7 were determined to be $1.85(\pm0.20)\times10^9$ $M^{-1}\cdot s^{-1}$ and $9.95(\pm0.26)\times10^9$ $M^{-1}\cdot s^{-1}$, respectively. Density functional theory was used to predict the main ozone reaction sites of 5-FU (olefin) and CAP (olefin and deprotonated secondary amine), and these mechanisms were supported by the identified transformation products. Carboxylic acids constituted a majority of the residual organic matter for 5-FU ozonation; however, carboxylic acids and aldehydes were important components of the residual organic matter generated by CAP. Ozone removed the toxicity of 5-FU to *Vibrio fischeri*, but the residual toxicity of ozonated CAP solutions exhibited an initial increase before subsequent removal. Ultimately, these results suggest that ozone is a suitable technology for treatment of 5-FU and CAP, although the residual toxicity of transformation products must be carefully considered.

✉ Corresponding author
E-mail: yg-den@mail.tsinghua.edu.cn

1 Introduction

Anticancer drugs (ADs) are extensively used in chemotherapy treatments for cancer patients to inhibit the malignant proliferation of cancer cells through cytostatic, cytotoxic, and antineoplastic mechanisms. Like most pharmaceuticals, ADs tend to enter the environment through the feces and urine of patients (Heath et al., 2016). The main sources are municipal wastewater, hospitals/clinics, pharmaceutical industries, and solid waste disposal sites (Zhang et al., 2013). As society ages, the incidence of cancer continues to increase (National Cancer Institute, 2018), leading to more consumption of ADs and causing pseudo-persistence of these compounds in select environments (Kümmerer et al., 2016;Deanna, 2018). Due to the carcinogenic, teratogenic, and mutagenic properties, ADs represent a potential risk to both ecological systems and human health (Besse et al., 2012; Li et al., 2016).

The most commonly used antimetabolite AD, 5-fluorouracil (5-FU), and its prodrug (i.e., the inactive compound that is metabolized into 5-FU), capecitabine (CAP), inhibit thymidylate synthetase and improperly replace pyrimidine bases to impede cell metabolism (Straub, 2009). The physicochemical properties of 5-FU and CAP are shown in Table S1 of the Supporting Information (SI). Because of their extensive usage (Besse et al., 2012; Kümmerer et al., 2016) and incomplete metabolism (i.e., 85% for 5-FU and 70% for CAP) (Oldenkamp et al., 2013), these two compounds have been detected in raw and treated wastewater. For example, 5-FU concentrations in hospital wastewater were $<$ 8.6–123.5 μg/L in Austria (Mahnik et al., 2004; Mahnik et al., 2007), $<$ 5–27 ng/L in Switzerland (Tauxe-Wuersch et al., 2006; Kovalova, 2009), and 35–92 ng/L in Slovenia (Kosjek et al., 2013). In raw wastewater from municipal wastewater treatment plants (WWTPs), 5-FU was reported at concentrations of 4.7–14 ng/L (Kosjek et al., 2013). Similarly, CAP has been reported at 0.4–1.3 μg/L in hospital wastewater (Gómez-Canela et al., 2014; Ferre-Aracil et al., 2016), 5.6–72.6 ng/L in WWTP influent (Negreira et al., 2013; Negreira et al., 2014), and 5.1–36.0 ng/L in WWTP effluent (Negreira et al., 2014). CAP concentrations of up to 20 ng/L have also been reported in surface water (Azuma et al., 2015).

The environmental occurrence of 5-FU and CAP raises serious concerns for ecological health. For example, 5-FU exhibits chronic toxicity to primary consumers in the aquatic food web, including *Ceriodaphnia dubia* (EC_{50}= 3.35 μg/L) (Parrella et al., 2014) and *Pseudomonas putida* (EC_{50}= 27 μg/L) (Zounková et al., 2007). Interestingly, mixtures containing 5-FU and β-lactam antibiotics have demonstrated synergistic effects on growth inhibition of *Escherichia coli*, *Proteus vulgaris*, and *Pseudomonas aeruginosa* (Ueda et al., 1983). CAP, which is excreted with its active metabolite (i.e., 5-FU), also inhibits the growth of *Selenastrum capricornutum* algae (EC_{50}= 2.0 mg/L) (Guo et al., 2015). Based on their environmental occurrence, increasing consumption trends, and potent pharmacological/toxicological activity, 5-FU and CAP have been identified as priority contaminants (Besse et al., 2012; Booker et al., 2014).

Previous studies have investigated the degradation of these important ADs in natural and engineered systems. Despite partial 5-FU transformation by solar photolysis, no change in biodegradability or toxicity was observed (Lin et al., 2013; Lutterbeck et al., 2016). Slow reaction kinetics have been reported for hydrolysis and biodegradation of CAP (Franquet-Griell et al., 2017). For these reasons, the overall removal efficiency of 5-FU and CAP is low in conventional WWTPs (Franquet-Griell et al., 2015). Recent work has, therefore, focused on treatment of 5-FU or other recalcitrant micropollutants using advanced processes, such as UV irradiation (Miolo et al., 2011; Gómez-Canela et al., 2017), UV/H_2O_2 advanced oxidation (Liu et al., 2018; Yin et al., 2018; Zhang et al., 2018), photocatalytic oxidation (Lin and Lin, 2014), Fenton reactions (Qian et al., 2014; Governo et al., 2017), and chlorination (Li et al., 2015). UV irradiation has also been explored for CAP (Kosjek et al., 2013); however, the aquatic toxicity increased during treatment, indicating the formation of potent transformation products (Guo et al., 2015). These results suggest that other reaction mechanisms are needed to safely remove the toxicity associated with ADs and their degradation products.

The reaction kinetics, mechanisms, and pathways of 5-FU and CAP have been understudied for ozonation, which has been successfully used to treat other micropollutants (Hopkins and Blaney, 2014; Bui et al., 2016; Hopkins et al., 2017) and chemotherapy agents (Blaney et al., 2019). We posit that the specificity of ozone reactions coupled to the general reactivity of $^{\bullet}$OH can reduce the toxicity of water/wastewater containing ADs. In fact, a previous study indicated that ozone treatment removed the toxicity of 5-FU as measured by the Ames test (Rey et al., 1999). Other researchers demonstrated significant degradation of 5-FU (Lin et al., 2015) and CAP (Nielsen et al., 2013; Ferre-Aracil et al., 2016) in hospital wastewater by ozone. While these studies suggest the feasibility for effective ozone treatment of 5-FU, CAP, and the corresponding toxicity, detailed reaction kinetics, mechanisms, and pathways have not been reported. Such information is critical to the design of treatment systems for hospitals, WWTPs, and drinking water treatment plants.

The objectives of this study were as follows: 1) to determine the specific reaction kinetics of 5-FU and CAP with ozone and $^{\bullet}$OH, which are produced during ozone decomposition; 2) to elucidate the ozone and $^{\bullet}$OH reaction mechanisms for 5-FU and CAP during ozonation and confirm the identity of transformation products using theory, kinetics data, and quantum chemical calculations;

3) to examine the composition of residual organic carbon derived from 5-FU and CAP degradation; and, 4) to evaluate the toxicity of ozonated solutions using *Vibrio fischeri* and the Toxicity Estimation Software Tool (TEST). The aggregate results of this study comprehensively describe the degradation of 5-FU and CAP during ozonation and provide the fundamental data needed to effectively remove these priority ADs in both drinking water and wastewater.

2 Materials and methods

2.1 Ozonation experiments

An overview of the chemicals and reagents is provided in Text S1 of the SI. All ozonation experiments were performed at room temperature (27°C±1°C) in a semi-batch reactor with constant water volume (250 mL) and continuous gas flow (Fig. S1 in the SI). The ozone/oxygen mixed gas stream was produced by an ozone generator (OL80F/DST, Ozone Services, Canada). Ozone detectors (IDEAL-2000, Ideal, USA) were used to measure gaseous ozone concentrations in the influent and effluent lines. The gas flow rate was maintained at 250 mL/min using a mass flow controller (D08-1/ZM, Sevenstar Electronics, China). Most experiments were performed using an inlet ozone gas concentration of 8 g/m^3, and these conditions achieved dynamic equilibrium at an aqueous ozone concentration of approximately 4.5 mg/L within 4 min. To maintain the pH, 10 mM sodium phosphate buffer was added to the solution. Water samples were collected at predetermined times, and 10 mM sodium thiosulfate (approximately 100×the aqueous ozone concentration) was immediately added to each sample to quench residual ozone and $^{\bullet}$OH. To characterize residual organic matter composition, multiple experiments (for specific ozonation times) were run to obtain the large volume samples needed for analysis of carboxylic acids, aldehydes, and total organic carbon (TOC). All experiments were performed in triplicate and data are reported as mean±standard deviation.

2.2 Determination of reaction rate constants

The apparent second-order rate constants of 5-FU (pH 5–11) and CAP (pH 5–10) with aqueous ozone were measured by competition kinetics (Hopkins and Blaney, 2014) using the setup described above. To scavenge hydroxyl radicals and isolate reactions with ozone, 30 mM *t*-BuOH was added to the solution. SMX was used as the competing species due to the availability of species-specific second-order rate constants. The rate constants of the cationic, neutral, and anionic SMX species with ozone are 1.71×10^5, 3.24×10^5, and 4.18×10^5 M$^{-1}\cdot$s^{-1}, respectively; note that the acid dissociation constants are $10^{-1.8}$ (K_{a1}) and $10^{-5.6}$ (K_{a2}) (Beltrán et al., 2009). With this information, the apparent rate constant for SMX reaction with ozone was calculated. For reaction kinetics of CAP with aqueous ozone in pH 5–7, phenol (i.e., $k''_{O_3,phenol} = 1.3\times10^4$ M$^{-1}\cdot$s^{-1}, $k''_{O_3,phenolate} = 1.4\times10^9$ M$^{-1}\cdot$s^{-1}; $pK_a = 9.9$) (Deborde et al., 2005) was used as the competing species.

The reaction rate constants of 5-FU and CAP with $^{\bullet}$OH were measured at room temperature (27°C±1°C) and pH 7 (10 mM phosphate buffer) through competition kinetics. Experiments were performed using the UV/H_2O_2 system, which produced $^{\bullet}$OH upon irradiation of an 80 mM H_2O_2 solution with 2.6 W UV light centered at 320±2 nm (half-band width, 12±2 nm). The second-order rate constant of the competing species, *p*CBA, with $^{\bullet}$OH ($k''_{\bullet OH,pCBA}$) is 5×10^9 M$^{-1}\cdot$s^{-1} at pH 7 (Buxton et al., 1988). The initial concentrations of *p*CBA and the ADs were set to 25 μM. To quench reactions in the UV/H_2O_2 system, 30 mM sodium thiosulfate was added to samples. All reaction kinetics experiments (i.e., ozone and $^{\bullet}$OH) were performed in triplicate, and 95% confidence intervals/bands were computed using OriginPro (OriginLab Corp., USA).

The second-order rate constants for 5-FU and CAP reaction with $^{\bullet}$OH were calculated using Eq. (1) (Jin et al., 2012).

$$k''_{\bullet OH,AD} = \frac{k'_{AD} - k'_{d,AD}\left(\frac{E'_{with\ H_2O_2}}{E'_{no\ H_2O_2}}\right)}{k'_{pCBA} - k'_{d,pCBA}\left(\frac{E'_{with\ H_2O_2}}{E'_{no\ H_2O_2}}\right)} k''_{\bullet OH,pCBA}. \quad (1)$$

In Eq. (1), $k''_{\bullet OH,AD}$ and $k''_{\bullet OH,pCBA}$ are the second-order rate constants for reaction of an AD and *p*CBA with $^{\bullet}$OH, respectively, k'_{AD} and k'_{pCBA} are the observed pseudo-first-order rate constants for degradation of an AD and *p*CBA in the UV/H_2O_2 system, respectively, $k'_{d,AD}$ and $k'_{d,pCBA}$ are pseudo-first-order rate constants for direct photolysis of an AD and *p*CBA, respectively, $E'_{with\ H_2O_2}$ is the average irradiance in solutions containing H_2O_2, and $E'_{no\ H_2O_2}$ is the average irradiance in solutions without H_2O_2.

To distinguish the contributions of aqueous ozone and $^{\bullet}$OH to the overall transformation of ADs, $^{\bullet}$OH exposure ($\int[^{\bullet}OH]\ dt$) was calculated with Eq. (2) (Lee et al., 2014).

$$\int_0^t [^{\bullet}OH]\ dt = -\frac{1}{k''_{\bullet OH,pCBA}} \ln\left(\frac{[pCBA]_t}{[pCBA]_0}\right). \quad (2)$$

In Eq. (2), $[pCBA]_0$ and $[pCBA]_t$ are the molar *p*CBA concentrations at time 0 and *t*, respectively. To prevent major changes in R_{ct} (Elovitz et al., 2000), which is the ratio of $^{\bullet}$OH exposure to O_3 exposure, the initial concentration of *p*CBA (2.5 μM) was an order of

magnitude lower than that of the ADs (50 μM). Experiments were performed at inlet ozone gas concentrations of 2, 8, and 13 g/m^3.

2.3 Analytical procedures

Concentrations of 5-FU, CAP, SMX, phenol, *p*CBA, and organic acids were measured by HPLC-UV (Prominence, Shimadzu, Japan). The *p*CBA probe was measured by HPLC (Ultimate 3000, Dionex, USA) with electrospray ionization tandem mass spectrometry (API3200, AB Sciex, USA). A hybrid quadrupole time-of-flight mass spectrometer (XEVO G2 QTOF, Waters, USA) was used to obtain the accurate mass of transformation products. The detailed information is provided in Text S2 and Table S2 of the SI. Aldehydes were derivatized using DNPH to form hydrazone compounds, extracted into methylene dichloride, and analyzed by HPLC-UV. The method details are available in Table S2 of the SI. TOC was measured with a TOC analyzer (TOC-VCPH, Shimadzu, Japan) (Zhao et al., 2017).

2.4 Quantum chemical calculations

Gaussian 09 software was employed for density functional theory calculations on 5-FU and CAP. The conformation optimization and frequency calculation of all molecules and corresponding ions were performed using B3LYP hybrid functional analysis with the 6-311 ++ G (d,p) basis set (Blicharska and Kupka, 2002; Mohamed et al., 2017). The polarizable continuum model with the integral equation formalism variant was used to calculate solvent effects. To inform initiation reactions of aqueous ozone and hydroxyl radicals with protonated/deprotonated 5-FU and CAP, the Fukui function was employed. It can reflect the change of electron density in different regions, so as to evaluate the reaction reactivity (Fu et al., 2014). Fukui function contour maps were visualized in the Gaussview software after conversion of the results with Multiwfn.

2.5 Assessment and estimation of toxicity

The luminescent bacterium *V. fischeri* has been used to measure toxicity of chemical contaminants and whole wastewater solutions easily, quickly, and reliably (Yu et al., 2014). Using standard protocols (ISO11348-2007), *V. fischeri* was employed to evaluate the acute toxicity of ozonated AD solutions. Luminescence was measured by photodetector (BHP9511, Hamamatsu Photonics, China) for 15-min contact times. Furthermore, TEST (version 4.2.1) was used to predict the acute toxicity of CAP and its transformation products on *Daphnia magna* by the consensus method, averaging the predicted toxicities from QSAR methodologies.

3 Results and discussion

3.1 Reaction kinetics of 5-FU and CAP

3.1.1 Ozone kinetics

Ozone reaction with 5-FU and CAP followed second-order kinetics as indicated by the competition kinetics data in Fig. S2 of the SI. To determine the specific reaction kinetics between ozone and protonated/deprotonated ADs, the apparent second-order rate constants for 5-FU and CAP reaction with ozone ($k''_{O_3,app}$) were measured for pH 5–11 and pH 5–10, respectively. These pH ranges were selected to account for 5-FU (pK_{a1}= 7.2; pK_{a2}= 12.0) (MarvinSketch, 2018) and CAP (pK_a= 8.8) (Kosjek and Heath, 2011) speciation. Figure 1 shows that the experimental values of $k''_{O_3,AD,app}$ varied with pH. The $k''_{O_3,5\text{-FU},app}$ value increased from 6.64×10^4 $M^{-1}\cdot s^{-1}$ at pH 5 to 3.72×10^6 $M^{-1}\cdot s^{-1}$ at pH 11. Similarly, $k''_{O_3,CAP,app}$ increased from 7.32×10^3 $M^{-1}\cdot s^{-1}$ at pH 5 to 3.76×10^5 $M^{-1}\cdot s^{-1}$ at pH 10. Ozone preferentially reacts with electron-rich moieties; therefore, the increase in $k''_{O_3,AD,app}$ likely stems from the deprotonation of the secondary amines in 5-FU and CAP (Sonntag et al., 2012). The $k''_{O_3,5\text{-FU},app}$ values were evaluated using the additive model shown in Eq. (3).

$$k''_{O_3,5\text{-FU},app} = \alpha_{5\text{-FU},0}\ k''_{O_3,5\text{-FU},0} + \alpha_{5\text{-FU},1}\ k''_{O_3,5\text{-FU},1} + \alpha_{5\text{-FU},2}\ k''_{O_3,5\text{-FU},2}. \quad (3)$$

In Eq. (3), $\alpha_{5\text{-FU},i}$ and $k''_{O_3,5\text{-FU},i}$ represent the ionization factors and specific second-order rate constants of the protonated and deprotonated 5-FU species; note that the 0, 1, and 2 labels indicate the fully protonated, singly deprotonated, and doubly deprotonated 5-FU species, respectively. The ionization factors are defined in Eqs. (4)–(6).

$$\alpha_{5\text{-FU},0} = \frac{1}{1 + 10^{(pH - pK_{a1})} + 10^{(2pH - pK_{a1} - pK_{a2})}}, \quad (4)$$

$$\alpha_{5\text{-FU},1} = \frac{1}{1 + 10^{(pK_{a1} - pH)} + 10^{(pH - pK_{a2})}}, \quad (5)$$

$$\alpha_{5\text{-FU},2} = \frac{1}{1 + 10^{(pK_{a1} + pK_{a2} - 2pH)} + 10^{(pK_{a2} - pH)}}. \quad (6)$$

A similar strategy was used to model $k''_{O_3,CAP,app}$ (Eqs. (7)–(9)).

$$k''_{O_3,CAP,app} = \alpha_{CAP,0}\ k''_{O_3,CAP,0} + \alpha_{CAP,1}\ k''_{O_3,CAP,1}, \quad (7)$$

$$\alpha_{CAP,0} = \frac{1}{1 + 10^{(pH - pK_a)}}, \quad (8)$$

$$\alpha_{\mathrm{CAP},1} = \frac{1}{1 + 10^{(\mathrm{pK}_a - \mathrm{pH})}}, \tag{9}$$

The apparent second-order rate constants and pK_a values for 5-FU were used in conjunction with Eqs. (3)–(6) to solve for the following specific second-order rate constants: $k''_{O_3,5\text{-FU},0}$, $7.07(\pm0.11)\times10^4$ $M^{-1}\cdot s^{-1}$; $k''_{O_3,5\text{-FU},1}$, $1.36(\pm0.06)\times10^6$ $M^{-1}\cdot s^{-1}$; and, $k''_{O_3,5\text{-FU},2}$, $2.62(\pm0.17)\times10^7$ $M^{-1}\cdot s^{-1}$. Similarly, the specific second-order rate constants were determined for ozone reaction with the protonated ($k''_{O_3,CAP,0} = 9.69(\pm0.08)\times10^3$ $M^{-1}\cdot s^{-1}$) and deprotonated ($k''_{O_3,CAP,1} = 4.28(\pm0.07)\times10^5$ $M^{-1}\cdot s^{-1}$) CAP species. The rate constants of the neutral and singly deprotonated 5-FU species are the same magnitude as previously reported values for structurally-similar thymine (Theruvathu et al., 2001). In addition, the rate constant of deprotonated 5-chlorouracil (i.e., 1.3×10^6 $M^{-1}\cdot s^{-1}$) was consistent with the monovalent 5-FU anion (Theruvathu et al., 2001). These specific rate constants were used with Eqs. (3) and (7), solution pH, and the pK_a values to construct the model curves for $k''_{O_3,AD,app}$ of 5-FU and CAP in Fig. 1. The additive kinetics model demonstrated a good fit to experimental data. Ultimately, 5-FU and CAP rapidly reacted with aqueous ozone at environmental pH, suggesting that ozone-based processes may be a viable solution for treating these ADs in water and wastewater.

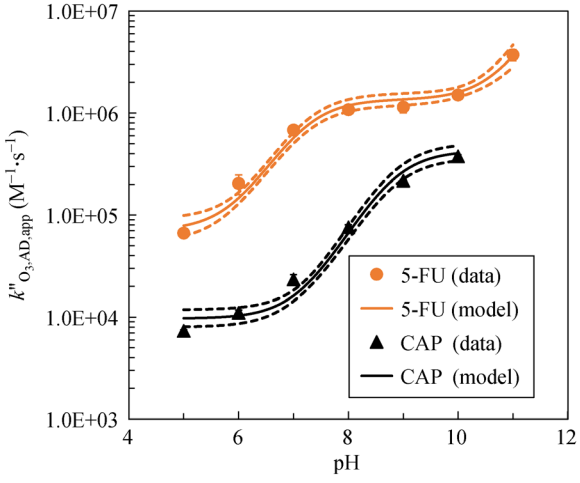

Fig. 1 Apparent second-order rate constants at 27°C±1°C for the reaction of aqueous ozone with 5-FU and CAP as a function of solution pH. The solid curves stem from Eq. (3) (5-FU) and (7) (CAP), and the dashed curves are 95% confidence bands.

3.1.2 Hydroxyl radical kinetics

The observed degradation of 5-FU, CAP, and *p*CBA in the UV and UV/H_2O_2 systems is shown as a function of time in Fig. S3 of the SI. A summary of the pseudo-first-order rate constants and the ratios of $E'_{\text{with } H_2O_2}$ to $E'_{\text{no } H_2O_2}$ for the 5-FU and CAP experiments is provided in Table S3 of the SI. Using Eq. (1) and the information in Table S3 of the SI, the apparent second-order rate constants for •OH reaction with 5-FU and CAP at pH 7 were calculated to be $1.85(\pm0.20)\times10^9$ $M^{-1}\cdot s^{-1}$ and $9.95(\pm0.26)\times10^9$ $M^{-1}\cdot s^{-1}$, respectively. As expected, these values are similar to rate constants for •OH reaction with other pharmaceuticals (Elovitz et al., 2008), reflecting the nonselective reaction mechanisms of •OH.

3.1.3 Contribution of ozone and hydroxyl radicals to AD transformation

To determine the relative importance of the ozone and hydroxyl radical transformation pathways for 5-FU and CAP, experiments were conducted using *p*CBA as a •OH probe. The change in 5-FU and CAP concentration is shown as a function of time in Fig. 2(a). Experimental results indicated that both 5-FU and CAP quickly degraded during ozonation; furthermore, 5-FU was transformed more quickly than CAP, as expected from the kinetic parameters reported above.

In the semi-batch reactor with constant water volume, the integrated mass balance on an AD is described by Eq. (10).

$$\ln\left(\frac{[\mathrm{AD}]_t}{[\mathrm{AD}]_0}\right) = k''_{O_3,AD,app} \int_0^t [O_3]\ dt + k''_{\bullet OH,AD,app} \int_0^t [\bullet OH]\ dt. \tag{10}$$

The contribution of hydroxyl radicals ($f_{\bullet OH}$) to the overall AD degradation can be expressed as Eq. (11).

$$f_{\bullet OH} = \frac{k''_{\bullet OH,AD,app} \int_0^t [\bullet OH]\ dt}{k''_{O_3,AD,app} \int_0^t [O_3]\ dt + k''_{\bullet OH,AD,app} \int_0^t [\bullet OH]\ dt}. \tag{11}$$

Eq. (11) can be modified through substitution of Eqs. (2) and (10), leading to Eq. (12).

$$f_{\bullet OH} = \frac{k''_{\bullet OH,AD,app} \ln\left(\frac{[p\mathrm{CBA}]_0}{[p\mathrm{CBA}]_t}\right)}{k''_{\bullet OH,p\mathrm{CBA},app} \ln\left(\frac{[\mathrm{AD}]_0}{[\mathrm{AD}]_t}\right)}. \tag{12}$$

The $f_{\bullet OH}$ values determined for 5-FU and CAP at different inlet ozone gas concentrations are reported in Fig. 2(b). No obvious trends in the $f_{\bullet OH}$ values for 5-FU or CAP were apparent, suggesting that the inlet ozone gas concentration had no effect on the relative contributions of ozone and •OH on AD transformation. For 5-FU, the $f_{\bullet OH}$ values were below 0.07, whereas the $f_{\bullet OH}$ values for CAP ranged from 0.28 to 0.60. These results indicate that direct

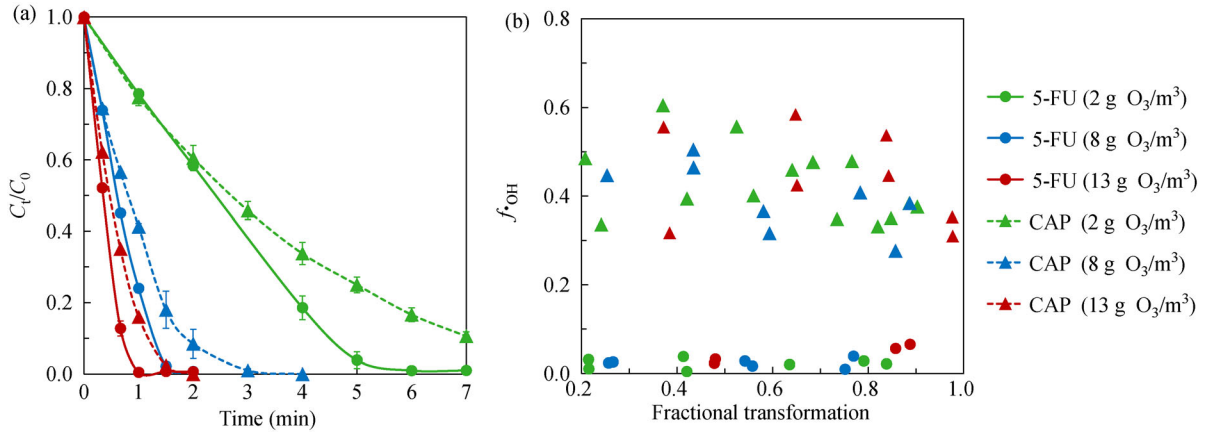

Fig. 2 (a) Normalized 5-FU and CAP concentrations as a function of ozonation time and (b) the contribution of hydroxyl radicals ($f_{\cdot OH}$) to transformation of 5-FU and CAP as a function of the overall 5-FU or CAP transformation for different inlet ozone gas concentrations (i.e., 2, 8, and 13 g O_3/m^3). The experimental conditions were as follows: temperature, 27°C±1°C; pH, 7 (10 mM phosphate buffer); initial *p*CBA concentration, 2.5 μM; and, initial AD concentration, 50 μM.

oxidation by ozone dominates the degradation kinetics for 5-FU; however, •OH mechanisms play an important role in CAP oxidation. For environmental pH, direct ozone oxidation serves as a major transformation mechanism for both compounds, and these results suggest that ozone-based processes show potential to successfully treat 5-FU and CAP in water and wastewater.

3.2 Transformation products and proposed mechanisms

3.2.1 Prediction of reaction sites

The Fukui function has been used to predict the reactive sites for various contaminants (Bao et al., 2018). Generally, sites with a larger Fukui value are considered more susceptible to reaction compared to other regions of the molecule. Using the finite difference approximation, the Fukui function can be unambiguously calculated for different situations (e.g., electrophilic attack, f^-, and radical attack, f^0). The Fukui contours of the protonated and deprotonated 5-FU and CAP species were visualized to identify the most likely sites for ozone and •OH reaction. In this case, the f^- and f^0 values were associated with the reactivity of a particular site with ozone and •OH, respectively. The f^- contour maps for the 5-FU neutral species (5-FU), monovalent anion (5-FU$^-$), and divalent anion (5-FU^{2-}) reported in Figs. 3(a), 3(c), and 3(e) suggest that the olefin group (1C = 3C) is the main reaction site for ozone. The 5N nitrogen atom was also indicated as a possible ozone attack site; however, no transformation products associated with such reactions were confirmed (see the following section). Considering the similarity of the Fukui contours, the prominent difference in ozone reactivity with 5-FU ($k''_{O_3,5\text{-FU},0} = 7.07(\pm0.11)\times10^4$ $M^{-1}\cdot s^{-1}$), 5-FU$^-$ ($k''_{O_3,5\text{-FU},1} = 1.36(\pm0.06)\times10^6$ $M^{-1}\cdot s^{-1}$), and 5-FU^{2-} ($k''_{O_3,5\text{-FU},2} = 2.62(\pm0.17)\times10^7$ $M^{-1}\cdot s^{-1}$) likely

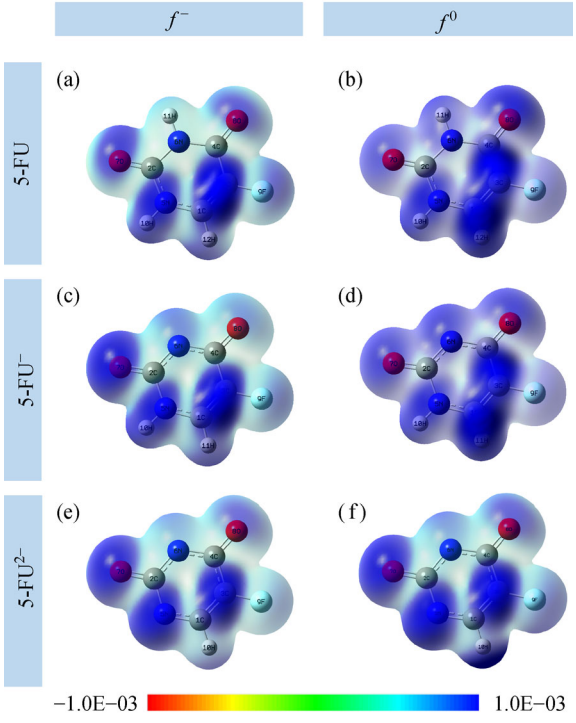

Fig. 3 Fukui contour maps with isovalue of 0.01 for the following: (a) f^- for 5-FU; (b) f^0 for 5-FU; (c) f^- for 5-FU$^-$; (d) f^0 for 5-FU$^-$; (e) f^- for 5-FU^{2-}; and, (f) f^0 for 5-FU^{2-}. The Fukui function parameters f^- and f^0 correspond to electrophilic O_3 attack and •OH attack, respectively.

stems from changes to the electron density of the ring, which includes the 1C = 3C olefin and the secondary amines, due to deprotonation reactions (Flyunt et al., 2002). Note that the atomic numbering system is shown in Fig. S4 of the SI. The 7O atom was also identified as a potential site for ozone reaction with 5-FU; however, no transformation products from the present study or previous

reports (Kosjek et al., 2013; Zhang et al., 2015) indicated ozone attack at this location, and the expected kinetics of ozone attack at the keto group are slow (Flyunt et al., 2002). Regardless of the 5-FU protonation state, the predicted reaction sites for •OH were focused on the olefin group (1C = 3C), as indicated in Figs. 3(b) (5-FU), 3(d) (5-FU^{-}), and 3(f) (5-FU^{2-}).

The f^{-} contours for the neutral CAP species shown in Fig. 4(a) suggest that ozone attacks the olefin group (1C = 2C). For the monovalent anion (CAP^{-}), the 27N secondary amine, which serves as the acid dissociation site of CAP, was identified as the preferred location for ozone attack due to the high f^{-} value (Fig. 4(c)). The large difference between the second-order rate constants for ozone reaction with CAP ($k''_{O_3,CAP,0} = 9.69(\pm 0.08)\times 10^3$ $M^{-1}\cdot s^{-1}$) and CAP^{-} ($k''_{O_3,CAP,1} = 4.28(\pm 0.07)\times 10^5$ $M^{-1}\cdot s^{-1}$) further suggests high ozone reactivity with the secondary amine. As above, the potential for ozone attack at the 8O keto group was not supported by experimental reaction kinetics or identified transformation products. For CAP, the expected •OH reaction sites were primarily associated with the heterocyclic ring (Fig. 4(b)), whereas the main reaction sites for CAP^{-} included the heterocycle and the deprotonated secondary amine (Fig. 4(d)).

3.2.2 Transformation products, mechanisms, and pathways

QTOF-MS was employed for the detection and identification of transformation products generated during ozonation of 5-FU and CAP. Molecular structures of the transformation products were proposed using the detected mass-to-charge ratios of the parent and fragment ions. Two transformation products were detected for 5-FU, and six products were observed for CAP (see Table S4 in the SI). For each AD, transformation products were labeled as "TP-" followed by the mass-to-charge ratio of the ion. These results, along with the reaction kinetics and Fukui predictions, were used to propose transformation pathways for ozonation of 5-FU (Fig. 5(a)) and CAP (Fig. 5(b)).

The identification of TP-195 and TP-159 reinforces the f^{-} Fukui predictions that the initial ozone attack on 5-FU, 5-FU^{-}, and 5-FU^{2-} occurs at the olefin group. Ozone reactions with olefins are well understood to follow the Criegee mechanism (Sonntag et al., 2012). As a strong electrophile, ozone reacts with the double bond to form the Criegee intermediate (Reaction 1 in Fig. 5(a)). The resulting ring is unstable and opens to form a zwitterion (Reaction 2). The zwitterion can react with the adjacent secondary amine and undergo defluorination to form TP-159 (Reaction 4). The hydrated zwitterion (Reaction 3), TP-195, can also form TP-159 through dehydration and defluorination (Reaction 5). For advanced oxidation, defluorination has been reported to involve substitution by hydrogen and hydroxyl groups (Wei et al., 2013). Based on observed transformation product mass-to-charge ratios, hydrogen substitution is proposed as the primary mechanism. Similar reactions (Reactions 1–5) have been reported for ozonation of thymine and thymidine (Flyunt et al., 2002). The f^{0} Fukui values predicted •OH attack at the olefin, but transformation products containing hydroxylated rings were not observed. This result may be attributed to the low (less than 7%) contribution of •OH to 5-FU transformation kinetics.

For CAP, four distinct reaction pathways were observed. The first pathway (Reactions 6–9 in Fig. 5(b)) is supported by the f^{-} values for CAP^{-} and identification of TP-245 and TP-203. In this case, ozone reacts with the free pair of

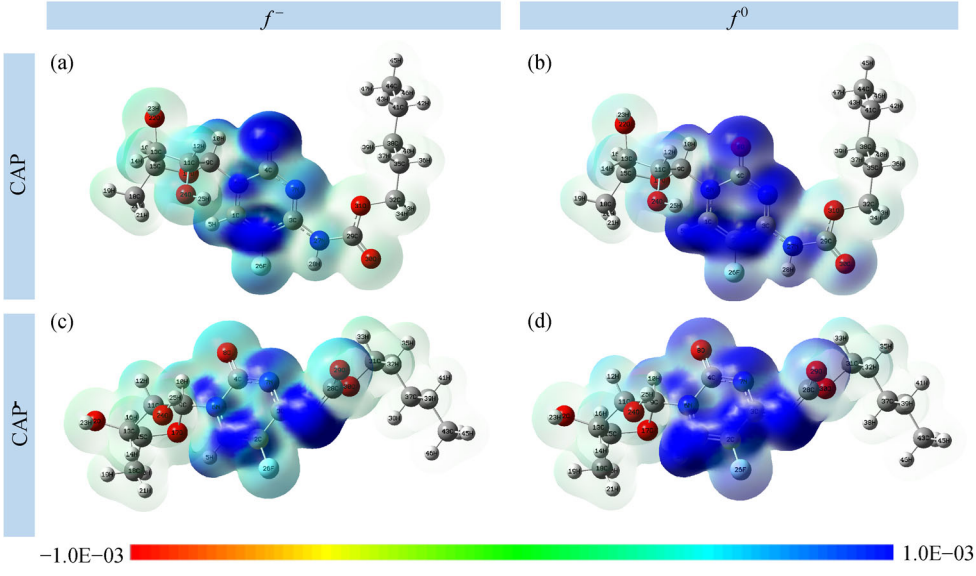

Fig. 4 Fukui contour maps with isovalue of 0.01 for the following parameters: (a) f^{-} for CAP; (b) f^{0} for CAP; (c) f^{-} for CAP^{-}; and, (d) f^{0} for CAP^{-}. The Fukui parameters f^{-} and f^{0} correspond to electrophilic O_3 attack and •OH attack, respectively.

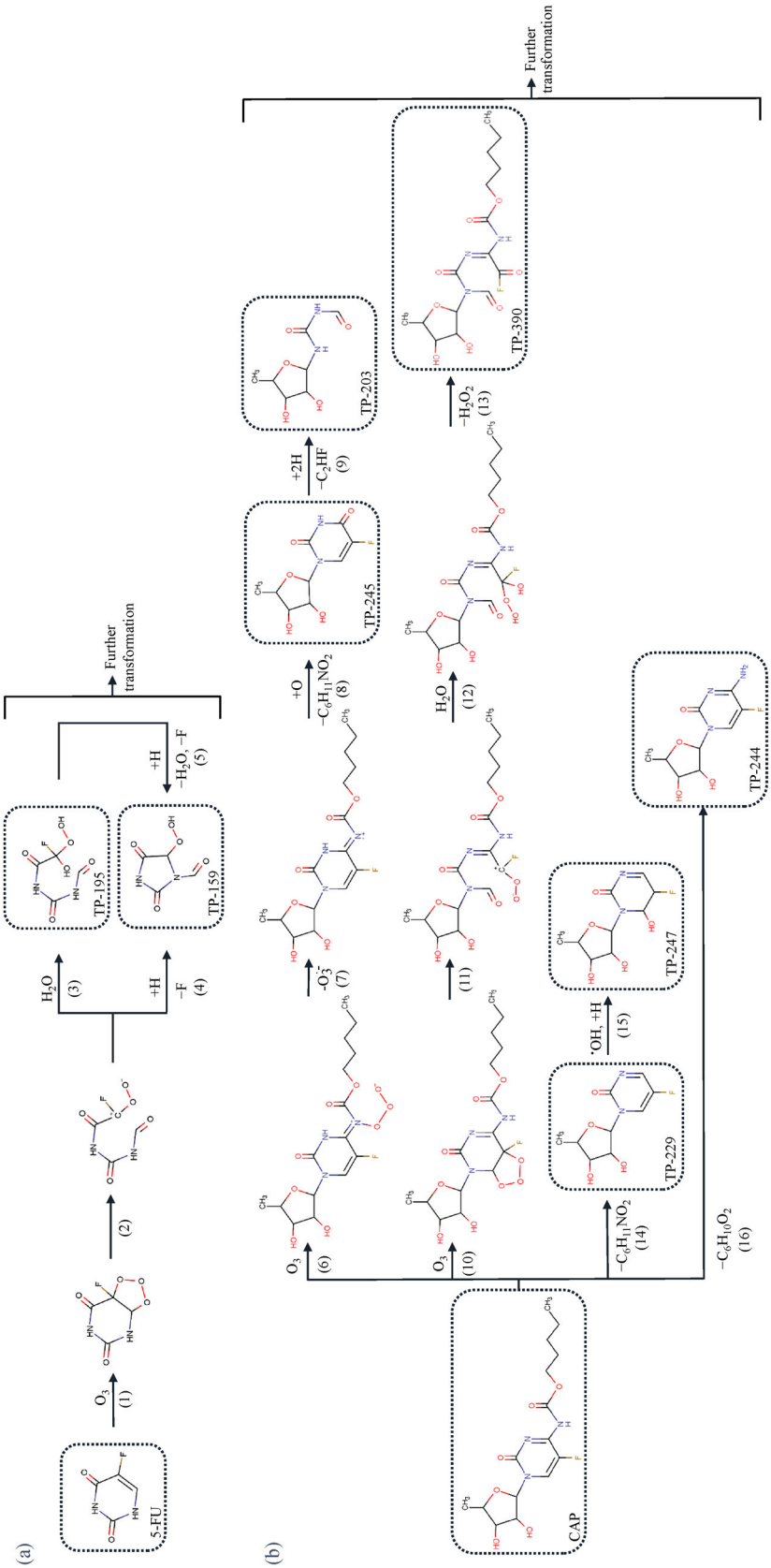

Fig. 5 Proposed reaction pathways for ozonation of (a) 5-FU and (b) CAP. Structures in the dashed boxes were confirmed by QTOF-MS.

electrons on the deprotonated secondary amine (Reaction 6). The resulting molecule is unstable and undergoes heterolytic cleavage of the ozone adduct to form an amine radical cation and an ozonide radical anion (Reaction 7). Subsequent decomposition reactions of the amine radical cation, similar to those reported for aliphatic amines (Sonntag et al., 2012), generate TP-245 (Reaction 8). Hydrolysis of TP-245 forms TP-203 (Reaction 9).

The f^- Fukui values of CAP and identification of TP-390 provide strong evidence for the second pathway (Reactions 10–13), which involves ozone attack at the olefin group (Reaction 10) followed by Criegee cleavage (Reaction 11). The loss of the hydroperoxide moiety produces TP-390 (Reaction 13) (Tekle-Röttering et al., 2016). The third pathway (Reactions 14–15) results in formation of TP-229 (Reaction 14) through cleavage of the C-N bond at the alkyl moiety, a mechanism that was previously reported for ozonation of fluoxetine (Zhao et al., 2017). Further reactions of TP-229 with •OH lead to hydroxylation of the olefin and generate TP-247 (Reaction 15) (Jin et al., 2017). The fourth reaction pathway involves •OH-mediated reactions at the protonated (neutral) amine of CAP. Unlike the third pathway, the amine moiety is retained by the molecule and TP-244 is formed (Reaction 16). The low reactivity of ozone with diazepam, phenytoin, and primidone support the proposed mechanism (Sonntag et al., 2012). Furthermore, •OH reactions were also identified at the amide bond during photocatalytic oxidation of 5-FU (Lin and Lin, 2014). The measured transformation products, Fukui analysis, and reaction mechanisms support CAP degradation in ozone-based processes at the olefin and secondary amine sites.

3.3 Characterization of other transformation products

Carboxylic acids and aldehydes have been frequently detected during ozone treatment and can impact the extent of contaminant mineralization (Chang et al., 2014). During degradation of 5-FU at pH 7, four carboxylic acids (i.e., formic acid, maleic acid, oxalic acid, and pyruvic acid) and formaldehyde were detected (Fig. 6(a)). The maximum concentrations of formic acid and maleic acid were observed after 2 min of ozonation and steadily declined following additional treatment. Similar production and

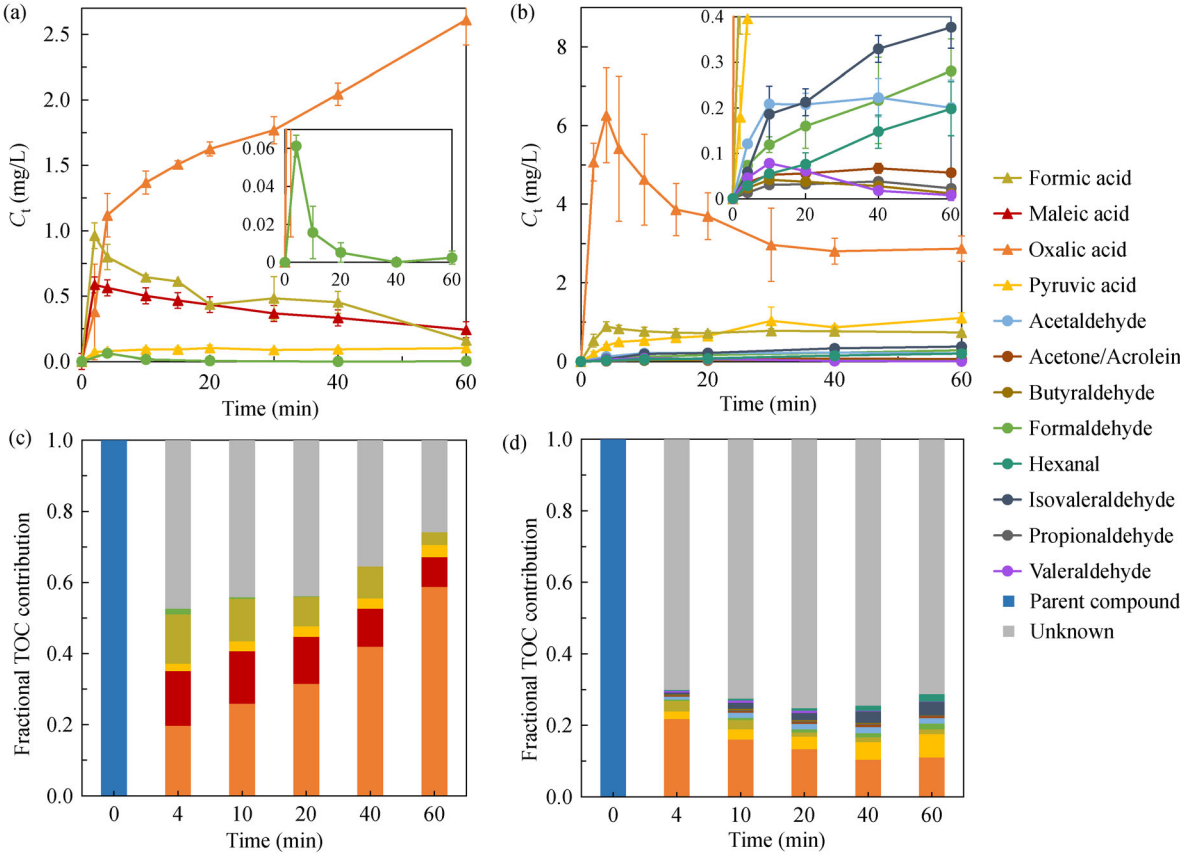

Fig. 6 Carboxylic acid and aldehyde concentrations during ozonation of (a) 5-FU and (b) CAP; fractional TOC contributions from ADs and other species for ozonation of (c) 5-FU and (d) CAP. The experimental conditions were as follows: inlet ozone gas concentration, 8 g O_3/m^3; temperature, 27°C±1°C; pH, 7 (10 mM phosphate buffer); and, initial concentration of parent compound, 50 μM. Acetone-DNPH and acrolein-DNPH had the same retention time and could not be separated. The color of the legend entries for (a) and (b) are also used in (c) and (d). The TOC removal for these experiments is plotted in Fig. S5 of the SI.

degradation trends for maleic acid were previously reported for ozone reaction at olefin moieties (Leitzke and Sonntag, 2009; Zhao et al., 2017). The concentration of oxalic acid rapidly increased during the first 4 min of ozonation and then continued to rise throughout the 60 min experiment but at a slower rate. The accumulation of oxalic acid likely stemmed from degradation of long-chain carboxylic acids, such as maleic acid, and the slow reaction of oxalic acid with ozone ($k''_{O_3,app} < 0.04\ M^{-1}\cdot s^{-1}$ at pH>5) (Faria et al., 2008). The pyruvic acid concentration slowly increased during the first 10 min of treatment and then demonstrated dynamic equilibrium for the next 50 min. Compared with the carboxylic acids, the concentration of formaldehyde was low (Fig. 6(a)). Formaldehyde is one of the most common byproducts in ozone systems, and aldehyde-based byproducts can be further oxidized (Chang et al., 2014). This behavior may explain the sharp increase and decrease in formaldehyde concentrations during 5-FU ozonation.

Three carboxylic acids (i.e., formic acid, oxalic acid, and pyruvic acid) and eight aldehydes (i.e., acetaldehyde, acetone/acrolein, butyraldehyde, formaldehyde, hexanal, isovaleraldehyde, propionaldehyde, and valeraldehyde) were detected during ozonation of CAP at pH 7 (Fig. 6 (b)). Unlike 5-FU ozonation, maleic acid was not produced from ozonation of CAP, which may inform the different trend in oxalic acid concentration. Even though the concentration of aldehydes was low compared to carboxylic acids, aldehydes tend to be more toxic (Zhao et al., 2017); therefore, the occurrence and fate of these species are critical to ensuring successful treatment of 5-FU and CAP. Ultimately, the generation of the various aldehydes suggests complex pathways for CAP degradation.

Even though the parent compounds were mostly transformed after 4 min of treatment at the 8 g O_3/m^3 inlet ozone gas concentration (Fig. 2(a)), the extent of mineralization was low for 5-FU (46%) and CAP (21%) after 60 min of treatment (see Fig. S5 in the SI). For ozonation of 5-FU, the contribution of carboxylic acids to the overall TOC continually increased to 74% over 60 min (Fig. 6(c)). Oxalic acid was the biggest contributor, comprising 59% of the residual TOC after 60 min of ozonation.

The trends in the composition of residual TOC differed for CAP (Fig. 6(d)). The fraction of aldehydes increased with ozonation. The contribution of carboxylic acids to the residual TOC first decreased and then increased. After 60 min of treatment, the contributions of carboxylic acids and aldehydes to TOC were 19% and 10%, respectively. The fraction of carboxylic acids in the residual TOC is expected to increase with further treatment due to low reactivity with ozone (Valsania et al., 2012) and continued transformation of aldehydes (Chang et al., 2014). The high fraction of unknown products (71% after 60 min of ozonation) and low mineralization demonstrate that, unlike 5-FU, CAP was transformed into complex products rather than small organic molecules.

3.4 Toxicity assessment

Ozonation can increase (Kuang et al., 2013) or decrease (Zhao et al., 2017) the toxicity of solutions containing pharmaceuticals. In some cases, the residual toxicity has been found to first increase and then decrease with further ozone exposure (Rosal et al., 2009; Gómez-Ramos et al., 2011; Cruz-Alcalde et al., 2017). In this study, the 15-min acute toxicity of partially treated solutions was assessed by luminescence inhibition of *V. fischeri* (Fig. 7(a)). For 5-FU, the residual toxicity of treated solutions fluctuated around 4% between 0 and 40 min of ozonation and then decreased to 1% after 60 min of ozone treatment. The TOC composition indicated that 5-FU byproducts were mostly

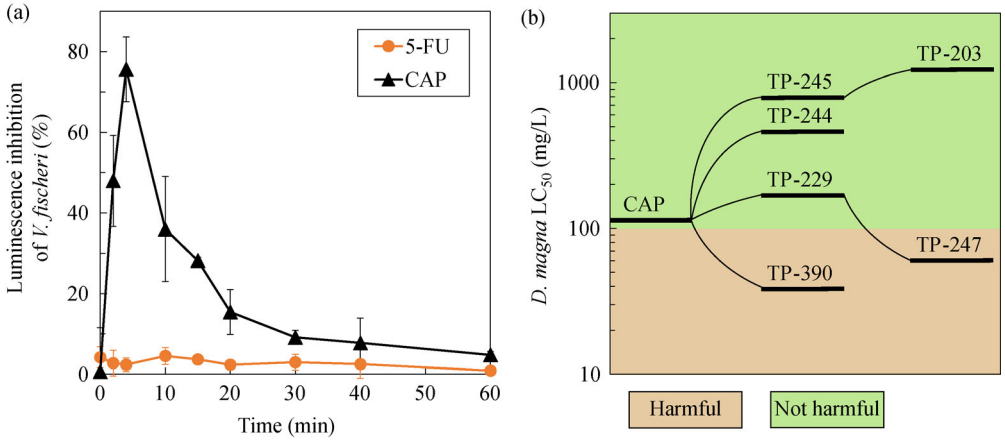

Fig. 7 (a) 15-min luminescence inhibition of *V. fischeri* for ozonated 5-FU and CAP solutions; (b) predicted 48-h LC_{50} for *D. magna* of CAP and its transformation products using the consensus method in the TEST software. Conditions for (a) were as follows: inlet ozone gas concentration, 8 g O_3/m^3; temperature, 27°C±1°C; pH, 7 (10 mM phosphate buffer); and, initial concentration of parent compound, 50 μM.

carboxylic acids, which are not expected to demonstrate toxicological activity. This scenario aligns with the observations in Fig. 7(a).

The untreated CAP solution exerted low toxicity on *V. fischeri* in agreement with previously reported data (Straub, 2009). Although CAP was rapidly transformed within 4 min (Fig. 2(a)), Fig. 7(a) indicates a considerable increase in toxicity for 0–20 min of ozonation. Similar findings were observed during UV irradiation of CAP (Guo et al., 2015). To further assess this residual toxicity pattern, the 48-h LC_{50} values of *D. magna* for CAP and its transformation products were predicted and classified (Chen et al., 2017) by the consensus method using the TEST software (Fig. 7(b)). The predicted toxicity to *D. magna* for most of the transformation products was lower than that of CAP. TP-247 and TP-390 were exceptions, potentially highlighting the role of these products in the increased residual toxicity observed for 0–20 min in Fig. 7 (a). The subsequent reduction of toxicity shows the detoxication of transformation products by ozonation; however, the luminescence inhibition of *V. fischeri* after 60 min of treatment (5%) is still higher than the initial condition (0.6%). These data suggest that toxic transformation products and aldehydes remain even after intensive ozone treatment (Zhao et al., 2017). To decrease the residual toxicity associated with these products, additional ozonation or an advanced oxidation polishing step, such as adding H_2O_2 to produce $^{\bullet}OH$ from the ozone residual, can be employed. Ultimately, these results indicate that ozone-based treatment provides rapid and effective treatment of 5-FU, but the transformation products of CAP need to be carefully evaluated to ensure removal of the associated toxicity.

4 Conclusions

The apparent reaction kinetics were measured for ozonation of 5-FU and CAP at pH 5–11. Furthermore, the specific second-order rate constants were determined for the reaction of aqueous ozone with 5-FU and CAP species, and these parameters varied across three orders of magnitude for 5-FU and two orders of magnitude for CAP. The reactivity increased for deprotonated 5-FU and CAP species. Like other pharmaceuticals, the apparent second-order rate constants for $^{\bullet}OH$ reaction with 5-FU and CAP at pH 7 were on the order of 10^9 $M^{-1}\cdot s^{-1}$. While both ozone and $^{\bullet}OH$ contributed to transformation of the ADs, ozone was the dominant mechanism for 5-FU and CAP. Quantum chemistry calculations suggested ozone attacks the olefin group in 5-FU and the olefin and deprotonated secondary amine in CAP. The transformation products and proposed reaction pathways supported these reaction mechanisms. The residual organic matter composition suggested that production of carboxylic acids during 5-FU transformation reduced the extent of mineralization. Ozonation of CAP generated aldehydes that comprised an important component of the residual organic matter. Ultimately, ozone was an effective method to treat 5-FU because the residual toxicity decreased with treatment; however, the residual toxicity of solutions containing CAP initially increased, suggesting the need for careful design of ozone reactors to ensure the removal of toxicity associated with transformation products.

Acknowledgements This work was supported by the Major Science and Technology Program for Water Pollution Control and Treatment in China (No. 2017ZX07202006), and Program for Changjiang Scholars and Innovative Research Team in University (No. IRT1261).

Electronic Supplementary Material Supplementary material is available in the online version of this article at https://doi.org/10.1007/s11783-019-1143-2 and is accessible for authorized users.

References

Azuma T, Ishiuchi H, Inoyama T, Teranishi Y, Yamaoka M, Sato T, Mino Y (2015). Occurrence and fate of selected anticancer, antimicrobial, and psychotropic pharmaceuticals in an urban river in a subcatchment of the Yodo River basin, Japan. Environmental Science and Pollution Research International, 22(23): 18676–18686

Bao Y, Deng S, Jiang X, Qu Y, He Y, Liu L, Chai Q, Mumtaz M, Huang J, Cagnetta G, Yu G (2018). Degradation of PFOA substitute: GenX (HFPO–DA Ammonium Salt): Oxidation with UV/Persulfate or reduction with UV/Sulfite? Environmental Science & Technology, 52(20): 11728–11734

Beltrán F J, Aguinaco A, García-Araya J F (2009). Mechanism and kinetics of sulfamethoxazole photocatalytic ozonation in water. Water Research, 43(5): 1359–1369

Besse J P, Latour J F, Garric J (2012). Anticancer drugs in surface waters: What can we say about the occurrence and environmental significance of cytotoxic, cytostatic and endocrine therapy drugs? Environment International, 39(1): 73–86

Blaney L, Lawler D F, Katz L E (2019). Transformation kinetics of cyclophosphamide and ifosfamide by ozone and hydroxyl radicals using continuous oxidant addition reactors. Journal of Hazardous Materials, 364: 752–761

Blicharska B, Kupka T (2002). Theoretical DFT and experimental NMR studies on uracil and 5-fluorouracil. Journal of Molecular Structure, 613(1–3): 153–166

Booker V, Halsall C, Llewellyn N, Johnson A, Williams R (2014). Prioritising anticancer drugs for environmental monitoring and risk assessment purposes. Science of the Total Environment, 473–474: 159–170

Bui X T, Vo T P, Ngo H H, Guo W S, Nguyen T T (2016). Multicriteria assessment of advanced treatment technologies for micropollutants removal at large-scale applications. Science of the Total Environment, 563–564: 1050–1067

Buxton G V, Greenstock C L, Helman W P, Ross A B (1988). Critical review of rate constants for reactions of hydrated electrons, hydrogen atoms and hydroxyl radicals ($\cdot$OH/$\cdot$O) in aqueous solution. Journal of Physical and Chemical Reference Data, 17(2): 513–886

Chang J, Chen Z L, Wang Z, Shen J M, Chen Q, Kang J, Yang L, Liu X W, Nie C X (2014). Ozonation degradation of microcystin-LR in aqueous solution: intermediates, byproducts and pathways. Water Research, 63: 52–61

Chen P, Wang F, Chen Z, Zhang Q, Su Y, Shen L, Yao K, Liu Y, Cai Z, Lv W, Liu G (2017). Study on the photocatalytic mechanism and detoxicity of gemfibrozil by a sunlight-driven TiO_2/carbon dots photocatalyst: The significant roles of reactive oxygen species. Applied Catalysis B: Environmental, 204: 250–259

Cruz-Alcalde A, Sans C, Esplugas S (2017). Priority pesticides abatement by advanced water technologies: The case of acetamiprid removal by ozonation. Science of the Total Environment, 599–600: 1454–1461

Deanna N (2018). Global Oncology Trends 2018. Parsippany: IQVIA Institute for Human Data Science

Deborde M, Rabouan S, Duguet J P, Legube B (2005). Kinetics of aqueous ozone-induced oxidation of some endocrine disruptors. Environmental Science & Technology, 39(16): 6086–6092

Elovitz M S, Shemer H, Peller J R, Vinodgopal K, Sivaganesan M, Linden K G (2008). Hydroxyl radical rate constants: comparing UV/H_2O_2 and pulse radiolysis for environmental pollutants. Journal of Water Supply: Research & Technology- Aqua, 57(6): 391–401

Elovitz M S, von Gunten U, Kaiser H (2000). Hydroxyl radical/ozone ratios during ozonation processes. II. The effect of temperature, pH, alkalinity, and DOM properties. Ozone Science and Engineering, 22(2): 123–150

Faria P C C, Órfão J J M, Pereira M F R (2008). Activated carbon catalytic ozonation of oxamic and oxalic acids. Applied Catalysis B: Environmental, 79(3): 237–243

Ferre-Aracil J, Valcárcel Y, Negreira N, de Alda M L, Barceló D, Cardona S C, Navarro-Laboulais J (2016). Ozonation of hospital raw wastewaters for cytostatic compounds removal. Kinetic modelling and economic assessment of the process. Science of the Total Environment, 556: 70–79

Flyunt R, Theruvathu J A, Leitzke A, von Sonntag C (2002). The reactions of thymine and thymidine with ozone. Journal of the Chemical Society, Perkin Transactions 2: Physical Organic Chemistry, 9: 1572–1582

Franquet-Griell H, Gómez-Canela C, Ventura F, Lacorte S (2015). Predicting concentrations of cytostatic drugs in sewage effluents and surface waters of Catalonia (NE Spain). Environmental Research, 138: 161–172

Franquet-Griell H, Medina A, Sans C, Lacorte S (2017). Biological and photochemical degradation of cytostatic drugs under laboratory conditions. Journal of Hazardous Materials, 323(Pt A): 319–328

Fu R, Tian L, Chen F (2014). Comparing methods for predicting the reactive site of electrophilic substitution. Wuli Huaxue Xuebao, 30(04): 628–639 (in Chinese)

Gómez-Canela C, Bolivar-Subirats G, Tauler R, Lacorte S (2017). Powerful combination of analytical and chemometric methods for the photodegradation of 5-Fluorouracil. Journal of Pharmaceutical and Biomedical Analysis, 137: 33–41

Gómez-Canela C, Ventura F, Caixach J, Lacorte S (2014). Occurrence of cytostatic compounds in hospital effluents and wastewaters, determined by liquid chromatography coupled to high-resolution mass spectrometry. Analytical and Bioanalytical Chemistry, 406(16): 3801–3814

Gómez-Ramos M M, Mezcua M, Agüera A, Fernández-Alba A R, Gonzalo S, Rodríguez A, Rosal R (2011). Chemical and toxicological evolution of the antibiotic sulfamethoxazole under ozone treatment in water solution. Journal of Hazardous Materials, 192(1): 18–25

Governo M, Santos M S F, Alves A, Madeira L M (2017). Degradation of the cytostatic 5-Fluorouracil in water by Fenton and photo-assisted oxidation processes. Environmental Science and Pollution Research International, 24(1): 844–854

Guo R, Zheng F, Chen J (2015). Evaluation of the aquatic toxic effect varied during the degradation of capecitabine under the environmental abiotic and biotic processes. RSC Advances, 5(94): 76772–76778

Heath E, Filipič M, Kosjek T, Isidori M (2016). Fate and effects of the residues of anticancer drugs in the environment. Environmental Science and Pollution Research International, 23(15): 14687–14691

Hopkins Z R, Blaney L (2014). A novel approach to modeling the reaction kinetics of tetracycline antibiotics with aqueous ozone. Science of the Total Environment, 468–469: 337–344

Hopkins Z R, Snowberger S, Blaney L (2017). Ozonation of the oxybenzone, octinoxate, and octocrylene UV-filters: Reaction kinetics, absorbance characteristics, and transformation products. Journal of Hazardous Materials, 338: 23–32

Jin L, Lü M, Zhao C, Min S, Zhang T, Zhang Q (2017). The reactivity of the 5-formylcytosine with hydroxyl radical: A theoretical perspective. Journal of Physical Organic Chemistry, 30(11): e3691

Jin X, Peldszus S, Huck P M (2012). Reaction kinetics of selected micropollutants in ozonation and advanced oxidation processes. Water Research, 46(19): 6519–6530

Kosjek T, Heath E (2011). Occurrence, fate and determination of cytostatic pharmaceuticals in the environment. TrAC Trends in Analytical Chemistry, 30(7): 1065–1087

Kosjek T, Perko S, Žigon D, Heath E (2013). Fluorouracil in the environment: Analysis, occurrence, degradation and transformation. Journal of Chromatography. A, 1290: 62–72

Kovalova L (2009).Cytostatics in the aquatic environment: Analysis, occurrence, and possibilities for removal. Dissertation for the Doctoral Degree. Aachen: RWTH Aachen University

Kuang J, Huang J, Wang B, Cao Q, Deng S, Yu G (2013). Ozonation of trimethoprim in aqueous solution: identification of reaction products and their toxicity. Water Research, 47(8): 2863–2872

Kümmerer K, Haiß A, Schuster A, Hein A, Ebert I (2016). Antineoplastic compounds in the environment-substances of special concern. Environmental Science and Pollution Research International, 23(15): 14791–14804

Lee Y, Kovalova L, McArdell C S, von Gunten U (2014). Prediction of micropollutant elimination during ozonation of a hospital wastewater effluent. Water Research, 64: 134–148

Leitzke A, Sonntag C V (2009). Ozonolysis of unsaturated acids in aqueous solution: Acrylic, methacrylic, maleic, fumaric and muconic acids. Ozone Science and Engineering, 31(4): 301–308

Li W, Nanaboina V, Chen F, Korshin G V (2016). Removal of polycyclic synthetic musks and antineoplastic drugs in ozonated wastewater: Quantitation based on the data of differential spectroscopy. Journal of Hazardous Materials, 304: 242–250

Li W, Tanumihardja J, Masuyama T, Korshin G (2015). Examination of

the kinetics of degradation of the antineoplastic drug 5-fluorouracil by chlorine and bromine. Journal of Hazardous Materials, 282: 125–132

Lin A Y, Hsueh J H, Hong P K A (2015). Removal of antineoplastic drugs cyclophosphamide, ifosfamide, and 5-fluorouracil and a vasodilator drug pentoxifylline from wastewaters by ozonation. Environmental Science and Pollution Research International, 22(1): 508–515

Lin A Y, Wang X H, Lee W N (2013). Phototransformation determines the fate of 5-fluorouracil and cyclophosphamide in natural surface waters. Environmental Science & Technology, 47(9): 4104–4112

Lin H H, Lin A Y (2014). Photocatalytic oxidation of 5-fluorouracil and cyclophosphamide via UV/TiO_2 in an aqueous environment. Water Research, 48: 559–568

Liu T, Yin K, Liu C, Luo J, Crittenden J, Zhang W, Luo S, He Q, Deng Y, Liu H, Zhang D (2018). The role of reactive oxygen species and carbonate radical in oxcarbazepine degradation via UV, UV/H_2O_2: Kinetics, mechanisms and toxicity evaluation. Water Research, 147: 204–213

Lutterbeck C A, Wilde M L, Baginska E, Leder C, Machado Ê L, Kümmerer K (2016). Degradation of cyclophosphamide and 5-fluorouracil by UV and simulated sunlight treatments: Assessment of the enhancement of the biodegradability and toxicity. Environmental Pollution, 208(Pt B): 467–476

Mahnik S N, Lenz K, Weissenbacher N, Mader R M, Fuerhacker M (2007). Fate of 5-fluorouracil, doxorubicin, epirubicin, and daunorubicin in hospital wastewater and their elimination by activated sludge and treatment in a membrane-bio-reactor system. Chemosphere, 66(1): 30–37

Mahnik S N, Rizovski B, Fuerhacker M, Mader R M (2004). Determination of 5-fluorouracil in hospital effluents. Analytical and Bioanalytical Chemistry, 380(1): 31–35

MarvinSketch (2018). MarvinSketch (version 18.23.0). Budapest: ChemAxon

Miolo G, Marzano C, Gandin V, Palozzo A C, Dalzoppo D, Salvador A, Caffieri S (2011). Photoreactivity of 5-fluorouracil under UVB light: Photolysis and cytotoxicity studies. Chemical Research in Toxicology, 24(8): 1319–1326

Mohamed H S, Dahy A A, Hassan G S, Eid S M, Mahfouz R M (2017). Quantum-chemical investigation on 5-fluorouracil anticancer drug. Structural Chemistry, 28(4): 1093–1109

National Cancer Institute (2018). Cancer Statistics. 2018. Bethesda: National Cancer Institute

Negreira N, de Alda M L, Barceló D (2014). Cytostatic drugs and metabolites in municipal and hospital wastewaters in Spain: filtration, occurrence, and environmental risk. Science of the Total Environment, 497–498: 68–77

Negreira N, López de Alda M, Barceló D (2013). On-line solid phase extraction-liquid chromatography-tandem mass spectrometry for the determination of 17 cytostatics and metabolites in waste, surface and ground water samples. Journal of Chromatography. A, 1280: 64–74

Nielsen U, Hastrup C, Klausen M M, Pedersen B M, Kristensen G H, Jansen J L C, Bak S N, Tuerk J (2013). Removal of APIs and bacteria from hospital wastewater by MBR plus O_3, O_3+ H_2O_2, PAC or ClO_2. Water Science & Technology, 67(4): 854–862

Oldenkamp R, Huijbregts M A J, Hollander A, Versporten A, Goossens H, Ragas A M J (2013). Spatially explicit prioritization of human antibiotics and antineoplastics in Europe. Environment International, 51: 13–26

Parrella A, Lavorgna M, Criscuolo E, Russo C, Fiumano V, Isidori M (2014). Acute and chronic toxicity of six anticancer drugs on rotifers and crustaceans. Chemosphere, 115: 59–66

Qian J, Li W, Zhang Y, Yun Y, Zhang Y (2014). Degradation of anticancer drug 5-fluorouracil by Fenton and oxalic-Fenton process. Environmental Chemistry, 33(7): 1229–1234 (in Chinese)

Rey R P, Padron A S, Leon L G, Pozo M M, Baluja C (1999). Ozonation of cytostatics in water medium. Nitrogen bases. Ozone Science and Engineering, 21(1): 69–77

Rosal R, Gonzalo M S, Boltes K, Letón P, Vaquero J J, García-Calvo E (2009). Identification of intermediates and assessment of ecotoxicity in the oxidation products generated during the ozonation of clofibric acid. Journal of Hazardous Materials, 172(2–3): 1061–1068

Sonntag C V, Gunten U V, Sonntag C V, Gunten U V (2012). Chemistry of Ozone in Water and Wastewater Treatment: from Basic Principles to Applications. London: Iwa Publishing

Straub J O (2009). Combined environmental risk assessment for 5-fluorouracil and capecitabine in Europe. Integrated Environmental Assessment and Management, 6(Suppl. 1): 540–566

Tauxe-Wuersch A, De Alencastro L F, Grandjean D, Tarradellas J (2006). Trace determination of tamoxifen and 5-fluorouracil in hospital and urban wastewaters. International Journal of Environmental Analytical Chemistry, 86(7): 473–485

Tekle-Röttering A, Reisz E, Jewell K S, Lutze H V, Ternes T A, Schmidt W, Schmidt T C (2016). Ozonation of pyridine and other N-heterocyclic aromatic compounds: Kinetics, stoichiometry, identification of products and elucidation of pathways. Water Research, 102: 582–593

Theruvathu J A, Flyunt R, Aravindakumar C T, von Sonntag C (2001). Rate constants of ozone reactions with DNA, its constituents and related compounds. Journal of the Chemical Society, Perkin Transactions 2, 3: 269–274

Ueda Y, Saito A, Fukuoka Y, Yamashiro Y, Ikeda Y, Taki H, Yasuda T, Saikawa I (1983). Interactions of beta-lactam antibiotics and antineoplastic agents. Antimicrobial Agents and Chemotherapy, 23(3): 374–378

Valsania M C, Fasano F, Richardson S D, Vincenti M (2012). Investigation of the degradation of cresols in the treatments with ozone. Water Research, 46(8): 2795–2804

Wei X, Chen J, Xie Q, Zhang S, Ge L, Qiao X (2013). Distinct photolytic mechanisms and products for different dissociation species of ciprofloxacin. Environmental Science & Technology, 47(9): 4284–4290

Yin K, Deng L, Luo J, Crittenden J, Liu C, Wei Y, Wang L (2018). Destruction of phenicol antibiotics using the UV/H_2O_2 process: Kinetics, byproducts, toxicity evaluation and trichloromethane formation potential. Chemical Engineering Journal, 351: 867–877

Yu X, Zuo J, Tang X, Li R, Li Z, Zhang F (2014). Toxicity evaluation of pharmaceutical wastewaters using the alga Scenedesmus obliquus and the bacterium Vibrio fischeri. Journal of Hazardous Materials, 266: 68–74

Zhang G, Liu C, Chen L, Hang T, Song M (2015). Identification of related substances in capecitabine by LC-MS. Chinese Journal of

New Drugs, 24(16): 1902–1910 (in Chinese)

Zhang J, Chang V W, Giannis A, Wang J Y (2013). Removal of cytostatic drugs from aquatic environment: A review. Science of the Total Environment, 445–446: 281–298

Zhang W, Zhou S, Sun J, Meng X, Luo J, Zhou D, Crittenden J (2018). Impact of chloride ions on UV/H_2O_2 and UV/persulfate advanced oxidation processes. Environmental Science & Technology, 52(13): 7380–7389

Zhao Y, Yu G, Chen S, Zhang S, Wang B, Huang J, Deng S, Wang Y (2017). Ozonation of antidepressant fluoxetine and its metabolite product norfluoxetine: Kinetics, intermediates and toxicity. Chemical Engineering Journal, 316: 951–963

Zounková R, Odráska P, Dolezalová L, Hilscherová K, Marsálek B, Bláha L (2007). Ecotoxicity and genotoxicity assessment of cytostatic pharmaceuticals. Environmental Toxicology and Chemistry, 26(10): 2208–2214